Polarisation charges and scattering behaviour of realistically rounded plasmonic nanostructures

T. V. Raziman and Olivier J. F. Martin*

Nanophotonics and Metrology Laboratory,
Swiss Federal Institute of Technology (EPFL), Lausanne, CH-1015, Switzerland

**olivier.martin@epfl.ch*

Abstract: We study the effect of realistically rounding nanorod antennae and gap antennae on their far field and near field properties. The simulations show that both scattering behaviour and polarisation charge distribution depend significantly on rounding. Rounding is also seen to have a major effect on coupling between nanostructures. The results suggest that it is important to incorporate the effect of rounding to be able to design plasmonic nanostructures with desired properties.

OCIS codes: (250.5403) Plasmonics; (240.6680) Surface plasmons; (000.4430) Numerical approximation and analysis.

References and links

1. S. A. Maier, *Plasmonics: Fundamentals and Applications* (Springer, 2007).
2. K. S. Yee, "Numerical solution of initial boundary value problems involving Maxwell's equations in isotropic media," IEEE Trans. Antennas Propag. **14,** 302–307 (1966).
3. A. Taflove and M. E. Brodwin, "Numerical solution of steady-state electromagnetic scattering problems using the time-dependent Maxwell's equations," IEEE Trans. Microwave Theory Tech. **23,** 623–630 (1975).
4. P. Monk, *Finite Element Methods for Maxwell's Equations* (Oxford University, 2003).
5. W.-H. Yang, G. C. Schatz, and R. P. Van Duyne, "Discrete dipole approximation for calculating extinction and Raman intensities for small particles with arbitrary shapes," J. Chem. Phys. **103,** 869–875 (1995).
6. O. J. F. Martin and N. B. Piller, "Electromagnetic scattering in polarizable backgrounds," Phys. Rev. E **58,** 3909–3915 (1998).
7. F. J. García de Abajo and A. Howie, "Retarded field calculation of electron energy loss in inhomogeneous dielectrics," Phys. Rev. B **65,** 115418 (2002).
8. U. Hohenester amd J. Krenn, "Surface plasmon resonances of single and coupled metallic nanoparticles: A boundary integral method approach," Phys. Rev. B **72,** 195429 (2005).
9. A. M. Kern and O. J. F. Martin, "Surface integral formulation for 3D simulations of plasmonic and high permittivity nanostructures," J. Opt. Soc. Am. **26,** 732–740 (2009).
10. M. E. Stewart, C. R. Anderton, L. B. Thompson, J. Maria, S. K. Gray, J. A. Rogers, and R. G. Nuzzo, "Nanostructured plasmonic sensors," Chem. Rev. **108,** 494–521 (2008).
11. X. Lu, M. Rycenga, S. E. Skrabalak, B. Wiley, and Y. Xia, "Chemical synthesis of novel plasmonic nanoparticles," Annu. Rev. Phys. Chem. **60,** 167–192 (2009).
12. A. M. Kern and O. J. F. Martin, "Excitation and reemission of molecules near realistic plasmonic nanostructures," Nano Lett. **11,** 482–487 (2011).
13. P. Mühlschlegel, H.-J. Eisler, O. J. F. Martin, B. Hecht, and D. W. Pohl, "Resonant optical antennas," Science **308,** 1607–1609 (2005).
14. S. Zhang, D. A. Genov, Y. Wang, M. Liu, and X. Zhang, "Plasmon-induced transparency in metamaterials," Phys. Rev. Lett. **101,** 047401 (2008).
15. N. Verellen, Y. Sonnefraud, H. Sobhani, V. V. Moshchalkov, P. Van Dorpe, P. Norlander, and S. A. Maier, "Fano resonances in coherent plasmonic nanocavities," Nano Lett. **9,** 1663–1667 (2009).
16. N. Liu, L. Langguth, T. Weiss, J. Kästel, M. Fleischhauer, T. Pfau, and H. Giessen, "Plasmonic analogue of electromagnetically induced transparency at the Drude damping limit," Nature Mater. **8,** 758–762 (2009).

#193624 - $15.00 USD Received 9 Jul 2013; revised 27 Aug 2013; accepted 29 Aug 2013; published 5 Sep 2013

17. R. Fuchs, "Theory of the optical properties of ionic crystal cubes," Phys. Rev. B **11,** 1732–1740 (1975).
18. M. A. Yurkin and M. Kahnert, "Light scattering by a cube: Accuracy limits of the discrete dipole approximation and the T-matrix method," J. Quant. Spectrosc. Radiat. Transfer **123,** 176–183 (2013).
19. W. J. Galush, S. A. Shelby, M. J. Mulvihill, A. Tao, P. Yang, and J. T. Groves, "A nanocube plasmonic sensor for molecular binding on membrane surfaces," Nano Lett. **9,** 2077–2082 (2009).
20. L. J. Sherry, S.-H. Chang, G. C. Schatz, R. P. Van Duyne, B. J. Wiley, and L. Xia, "Localized surface plasmon resonance spectroscopy of single silver nanocubes," Nano Lett. **5,** 2034–2038 (2005).
21. M. Rycenga, J. M. McLellan, and Y. Xia, "Controlling the assembly of silver nanocubes through selective functionalization of their faces," Adv. Mater. **20,** 2416–2420 (2008).
22. H. Chen, Z. Sun. W. Ni, K. C. Woo, H.-Q. Lin, L. Sun, C. Yan, and J. Wang, "Plasmon coupling in clusters composed of two-dimensionally ordered gold nanocubes," Small **5,** 2111–2119 (2009).
23. W. Li, P. H. C. Camargo, X. Lu, and Y. Xia, "Dimers of silver nanospheres: facile synthesis and their use as hot spots for surface-enhanced Raman scattering," Nano Lett. **9,** 485–490 (2009).
24. M. Rycenga, C. M. Cobley, J. Zeng, W. Li, C. H. Moran, Q. Zhang, D. Qin, and Y. Xia, "Controlling the synthesis and assembly of silver nanostructures for plasmonic applications," Chem. Rev. **111,** 3669–3712 (2011).
25. N. Grillet, D. Manchon, F. Bertorelle, C. Bonnet, M. Broyer, E. Cottancin, J. Lermé, M. Hillenkamp, and M. Pellarin, "Plasmon coupling in silver nanocube dimers: Resonance splitting induced by edge rounding," ACS Nano **5,** 9450–9462 (2011).
26. M. B. Cortie, F. Liu, M. D. Arnold, and Y. Niidome, "Multimode resonances in silver nanocuboids," Langmuir **28,** 9103–9112 (2012).
27. P. B. Johnson and R. W. Christy, "Optical constants of the noble metals," Phys. Rev. B **6,** 4370–4379 (1972).
28. A. M. Kern and O. J. F. Martin, "Pitfalls in the determination of optical cross sections from surface integral equation simulations," IEEE Trans. Antennas Propag. **58,** 2158–2161 (2010).
29. S. Zhang, K. Bao, N. J. Halas, H. Xu, and P. Norlander, "Substrate-induced fano resonances of a plasmonic nanocube: a route to increased-sensitivity localized surface plasmon resonance sensors revealed," Nano Lett. **11,** 1657–1663 (2011).
30. A. Unger and M. Kreiter, "Analysing the performance of plasmonic resonators for dielectric sensing," J. Phys. Chem. C **113,** 12243–12251 (2009).
31. A. Lovera, B. Gallinet, P. Norlander, and O. J. F. Martin, "Mechanisms of Fano resonances in coupled plasmonic systems," ACS Nano **7,** 4527–4536 (2013).

1. Introduction

Nanostructures with plasmonic resonances have found applications in chemical and biological sensing and various other fields [1]. In order to design nanostructures with desired plasmonic properties, it is necessary to be able to simulate their optical response with high accuracy. Various numerical techniques have been used to this end. Finite difference time domain (FDTD) [2, 3] and finite element method (FEM) [4] solve Maxwell's equations in the differential form in the time domain and frequency domain, respectively. These methods have the disadvantage that they require both the scatterer and the background volume to be discretised. To overcome this, integral equation methods have been proposed, which solve Maxwell's equations in the integral form. Discrete dipole approximation (DDA) [5] and volume integral equation (VIE) [6] require discretising the entire scatterer volume whereas boundary element method (BEM) [7, 8] and surface integral equation (SIE) [9] require only the discretisation of the scatterer boundary.

To achieve accurate agreement with the experimental behaviour of nanostructures, it is not merely enough to have an accurate simulation routine; it is equally important that the object being simulated represents the actual nanostructure accurately. Even though we would like to design ideal nanostructures, fabrication processes introduce various non-idealities [10, 11]. In particular, nanostructure surfaces become rough and geometric edges and corners end up being rounded to various degrees. The simulation needs to incorporate such fabrication induced non-idealities of the geometry. Comparing the behaviour of realistic nanostructures with their ideal counterparts shows significant differences [12].

Nanocuboids are the building blocks of many complicated nanostructures used widely in sensing applications, such as gap antennae [13] and Dolmen structures [14–16]. The existence of a high number of discrete symmetries makes cubes particularly interesting [17,18], and hence

#193624 - $15.00 USD Received 9 Jul 2013; revised 27 Aug 2013; accepted 29 Aug 2013; published 5 Sep 2013

nanocubes and nanocube assemblies have been subject to experimental study as well [19–22]. The different fabrication techniques [20–24] for such cuboidal and cubic nanostructures always introduce rounding effects, as visible in Fig. 1. This rounding gives rise to the prospect of changing the optical response of the structures significantly [20, 25, 26]. In this paper, we study the effect of rounding the edges and corners of cuboidal antennae and cuboidal gap antennae on their scattering behaviour as well as the induced polarisation charge distributions on their surfaces.

2. Formulation of the problem

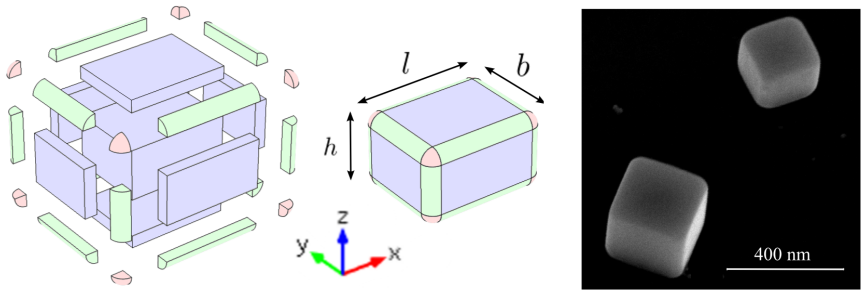

Fig. 1. *(Left)* The individual pieces which can be used to assemble the rounded cuboid. The cuboids, quarter-cylinders and sphere-octants have been coloured blue, green and red, respectively. *(Centre)* The rounded cuboid formed from the constituents. *(Right)* SEM image of silver nanocubes.

In this paper, the following procedure was used for rounding the corners and edges of cuboids uniformly. Consider a cuboid with dimensions l, b, h. Suppose we need to round the edges and corners with a rounding radius of r such that $2r \leq \min(l, b, h)$. This can be done ensuring continuity and differentiability of the surfaces by making a composite structure consisting of seven cuboids, twelve quarter-cylinders and eight sphere-octants. The assembly of a rounded cuboid from these pieces is shown in Fig. 1. It is easy to verify that all boundaries between meeting surfaces are smooth.

In all the structures considered here, the YZ plane cross section of the cuboids was kept constant as $b = h = 40$ nm while the length l along the X dimension of the structures and the radius of rounding r were varied. In the case of the gap antenna, two such identical cuboids were placed symmetrically such that their YZ-plane surfaces faced each other. In all the simulations presented here, a plane wave propagating in the Z direction and polarised along X was used for illuminating the structures. The nanostructures being simulated are made out of silver, unless explicitly mentioned otherwise. The dielectric function for silver was taken from Johnson and Christy [27].

The optical response of the nanostructures are simulated using the Surface Integral Equation (SIE) formulation [9]. The surface of each structure is discretised into a sufficient number of triangles to ensure numerical convergence for the solutions. The average area of a triangular mesh element was kept as approximately 5 nm^2 for all simulations.

Scattering cross section was calculated by evaluating the flux of scattered Poynting vector on a sphere centred at the structure and having a radius of 50 μm, and normalising the result to the incident field intensity:

$$C_{sc} = \frac{\oint \frac{1}{2} Re\left[\mathbf{E}_{sc} \times \mathbf{H}_{sc}^{*}\right] \cdot d\mathbf{S}}{\left|\frac{1}{2} Re\left[\mathbf{E}_{in} \times \mathbf{H}_{in}^{*}\right]\right|} \tag{1}$$

#193624 - $15.00 USD Received 9 Jul 2013; revised 27 Aug 2013; accepted 29 Aug 2013; published 5 Sep 2013

For this, scattered electric and magnetic fields were calculated at 1050 nearly equidistant points on the sphere [28]. Bisection method was used to locate peak scattering wavelength with high accuracy. Polarisation charges were calculated at the structure surfaces from the discontinuity in the normal component of electric field on either side of the surface:

$$\sigma_p = \frac{\mathbf{E}_{out} - \mathbf{E}_{in}}{\varepsilon_0} \cdot \hat{n}\,. \tag{2}$$

This was performed by subdividing the surface mesh into smaller triangles and evaluating the electric field 1 nm away from the centre of the triangles in either direction of the surface normal.

3. Results and discussion

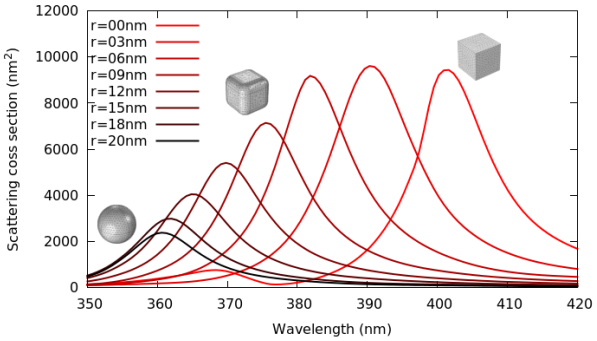

Fig. 2. Scattering cross section as a function of wavelength for various rounding radii (r) of the cube.

Consider a silver cube with a side length of 40 nm. Figure 2 shows the effect of rounding on the scattering cross section of the cube. It can be noted that the scattering plots exhibit a regular trend on increasing rounding radii. As the cube is gradually deformed into a sphere by increasing the rounding radius, two major changes occur: The wavelength at which peak scattering cross section is obtained blue shifts significantly while the peak value of the scattering cross section decreases to about one-fifth of the original value.

To understand what happens in the near field at the nanocubes for various radii of rounding, we look at the polarisation charges at the surface. The results are shown in Fig. 3. For the nanocube rounded only by 3 nm, the polarisation charges are heavily concentrated at the corners. This is akin to the lightning rod effect. As the rounding radius increases, the size of

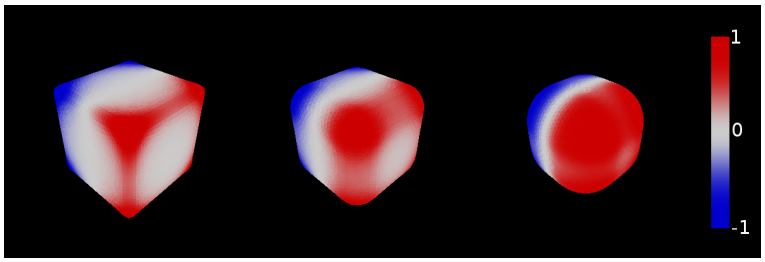

Fig. 3. Normalised polarisation charges on the surface of rounded nanocubes. *From left to right:* Rounding radius of 3 nm, 9 nm, 15 nm.

#193624 - $15.00 USD Received 9 Jul 2013; revised 27 Aug 2013; accepted 29 Aug 2013; published 5 Sep 2013

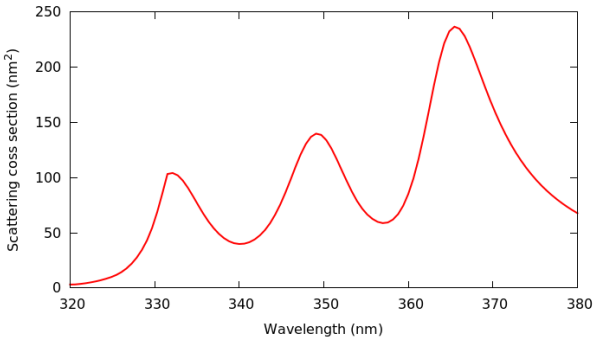

Fig. 4. Scattering cross section as a function of wavelength for a silver cuboid of 20 nm length, 40 nm $\times$ 40 nm cross section and rounding radius of 4 nm

the "corner" increases as well. As a result, the charges become less localised, and spread to the edges and faces of the rounded nanocube.

The numerical accuracy of the surface integral method and the computational tool has been validated many times for different structures [9,12,28]. The continuous shifting of the scattering peaks also suggests that there are no numerical problems arising due to the sharpness in the cube geometry. For additional validation, we performed analytical calculations using Mie theory for the case of the sphere and found perfect agreement in the location of the scattering peak. There is no such analytical treatment possible for a cube. However, various numerical methods have been used to calculate the scattering cross sections of cubes of different sizes and they have found the dominant scattering mode of the cube to be corner charge dominated. The value of scattering peak wavelength we calculated for the cube agrees well with those predicted in literature [17, 26, 29].

The trend of lower wavelength scattering peaks being associated with more spread-out charge distributions was also noticed in individual structures with multiple scattering peaks. As an example, consider a thin nanocuboid of dimensions 20 nm $\times$ 40 nm $\times$ 40 nm rounded to a radius of 4 nm. This structure has three prominent scattering cross section peaks occurring with a wavelength separation of about 20 nm, as shown in Fig. 4. The polarisation charges corresponding to the three scattering peaks have been shown in Fig. 5. There is significant difference between the charge profiles for the three cases. The lowest wavelength peak has polarisation charges distributed all over the square faces whereas the highest wavelength peak has the charges concentrated at the corners. The scattering peak at the intermediate wavelength has charges concentrated pri-

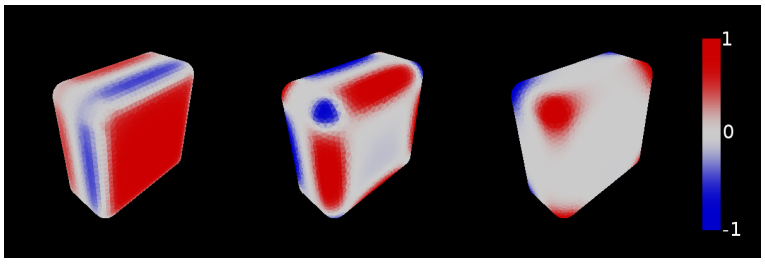

Fig. 5. Normalised polarisation charges on the surface of the 20 nm $\times$ 40 nm $\times$ 40 nm antenna for the three scattering peaks in Fig. 4. The figures, from left to right, correspond to the peaks from left to right, respectively.

#193624 - $15.00 USD Received 9 Jul 2013; revised 27 Aug 2013; accepted 29 Aug 2013; published 5 Sep 2013

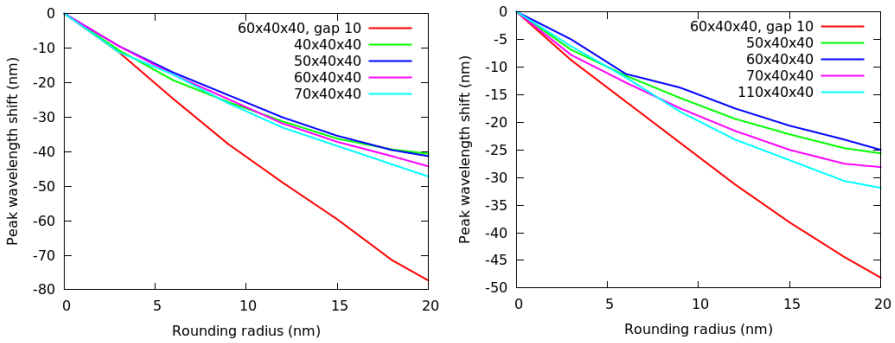

Fig. 6. The peak wavelength shift relative to an ideal structure for various values of rounding radii for (*Left*) Silver and (*Right*) Gold.

marily at the edges. Once again, the bluer scattering peak is seen to be associated with the more spread-out charge distribution. This correlation between spreading of charge and blue shifting of scattering peak needs to be studied further. However, we believe that the spreading of charges due to the reduction in the lightning rod effect might be what causes the blue shift of scattering peak on rounding nanostructures.

The peak shifting behaviour for cuboids of various lengths as well as gap antennae was studied in the same fashion. This time, cuboids made of silver as well as gold were considered. Dielectric function for gold was obtained from Johnson and Christy as well [27]. The trend of blue shifting of the scattering peak as a result of rounding was found in all studied structures made of gold and silver. The peak shift (relative to the scattering peak of ideal structures) as a function of rounding radius is presented in Fig. 6.

Interestingly, cuboids of different lengths show similar trends of blue shifting of peak wavelength on rounding. However, the gap antenna shows a significantly higher blue shift. The reason for the same can be understood by comparing the polarisation charge distributions for the peak scattering wavelengths of a single cuboid and that of a gap antenna. The polarisation charges for a single 60 nm $\times$ 40 nm $\times$ 40 nm nanorod ($r = 3$ nm) and that for an arm of a gap antenna formed by two such nanorods separated by 10 nm ($r = 3$ nm and $r = 9$ nm) are plotted in Fig. 7. As expected, for the single cuboid, the polarisation charges are concentrated at the corners. However, for the gap antenna, the charges are seen to be spread all over the surface facing the gap. This can be explained by the fact that there is an opposite charge at the match-

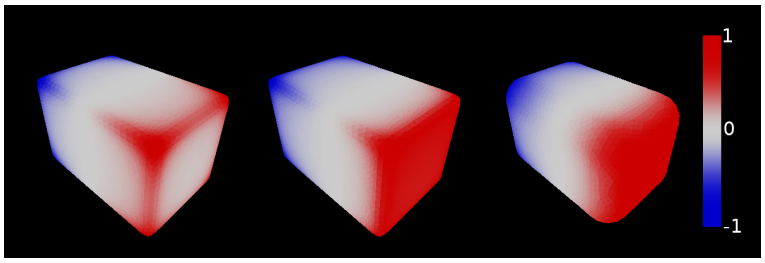

Fig. 7. Normalised polarisation charges at the peak scattering wavelength for *(Left)* a single 60 nm $\times$ 40 nm $\times$ 40 nm cuboid with a rounding radius of 3 nm and the gap-facing surface of a *(Centre)* gap antenna with two such cuboids separated by 10 nm and *(Right)* a similar gap antenna but with a rounding of 9 nm.

#193624 - $15.00 USD Received 9 Jul 2013; revised 27 Aug 2013; accepted 29 Aug 2013; published 5 Sep 2013

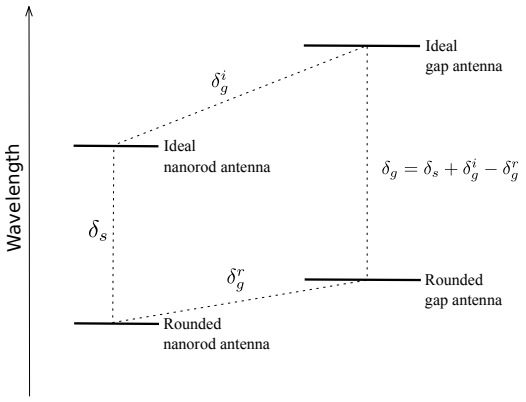

Fig. 8. The relationship between various wavelength shifts.

ing face of the other arm of the gap antenna, attracting charge on this arm towards it. The two oppositely charged faces with charges almost uniformly spread over them acts as a capacitor, providing high field coupling between the faces. However, when the rounding of the cuboids is increased, the situation changes. The polarisation charges are still attracted towards the gap face, but are now more dispersed around the curved edges. It is important to note that the flat part of the face is what is closest to the other antenna arm, thus providing maximum coupling. The presence of charges away from the flat region on the edges reduces the coupling.

This reduction in coupling is what results in a larger blue shift on rounding gap antennae as compared to rounding single cuboids. Consider a cuboid being rounded from an ideal shape to a maximally rounded shape. This would result in a blue shift of peak scattering wavelength by a value as seen earlier, call this shift δ_s. Now consider making a gap antenna out of two such identical ideal cuboids separated by d. Due to the field coupling between the two arms, the peak scattering wavelength for the ideal gap antenna is red shifted with respect to the peak for the ideal rod antenna by a value δ_g^i. Similarly, the peak scattering wavelength for the rounded gap antenna at the same separation d is red shifted with respect to the peak for the rounded rod antenna by a value δ_g^r. Since the coupling in the case of the rounded gap antenna is less than that of the ideal gap antenna, we expect $\delta_g^r < \delta_g^i$. The shift between the peak scattering wavelengths of the rounded gap antenna and the ideal gap antenna is given, as illustrated in Fig. 8, by $\delta_g = \left(\delta_s + \delta_g^i - \delta_g^r\right)$. Since $\delta_g^i > \delta_g^r$, we obtain that $\delta_g > \delta_s$. That is, the rounding induced blue shift is higher for a gap antenna as compared to a single cuboid antenna.

4. Conclusion

It has been shown that rounding affects the scattering from nanoantennae significantly. Since the far field scattering properties change as well, this is not merely a near field effect and will thus change any experimental parameters of the system. The difference is particularly significant for gap antennae, where peak scattering wavelength has been shown to shift by up to 80 nm in the case of Silver. This should be taken into consideration while simulating nanostructures to be fabricated to have desired properties. Fabrication always introduces rounding effects into structures, which must be estimated reasonably well and incorporated into the simulations so that the fabricated structures behave as expected. Since peak scattering wavelength is a regularly used quantity for sensing applications, the effect of rounding can be significant in those applications [30, 31]. Rounding effects also need to be considered in other problems where

#193624 - $15.00 USD Received 9 Jul 2013; revised 27 Aug 2013; accepted 29 Aug 2013; published 5 Sep 2013

coupling between surfaces plays a significant role, as similar to the case of the gap antenna, coupling can be reduced due to curvature in such cases as well.

Acknowledgments

It is a pleasure to acknowledge stimulating discussions with Shourya Dutta-Gupta on the topic. Thanks are also due to Martin Pfeiffer and Christian Santschi for providing the SEM image of the fabricated nanocubes, and to Jérémy Butet for helping with the Mie theory calculations. Funding from the Swiss National Science Foundation (Project 200020_135452) is gratefully acknowledged.

#193624 - $15.00 USD Received 9 Jul 2013; revised 27 Aug 2013; accepted 29 Aug 2013; published 5 Sep 2013